BEHAVIOR-BASED ADHESION CONTROL SYSTEM FOR SAFE ADHERENCE OF WALL-CLIMBING ROBOTS

D. SCHMIDT* and K. BERNS

Robotics Research Lab, University of Kaiserslautern, Kaiserslautern, Germany
**E-mail: dschmidt@cs.uni-kl.de*
http://agrosy.cs.uni-kl.de/cromsci

Safe adhesion is a large research area in the field of climbing robots. Many robotic systems use well-known magnetic adhesion or mechanical connections like claws, some others use classic closed-loop controllers in combination with negative pressure adhesion to ensure operation safety. This paper will introduce important safety aspects of the climbing robot CROMSCI which has a negative pressure system, an adaptive inflatable sealing and an omni-directional drive. We will illustrate the novel behavior-based closed-loop controller architecture which has different control levels — starting from individual chamber pressure controllers up to an overall force control. Experimental results will show the performance of the complete behavioral network.

Keywords: Climbing Robot, Behavior-Based Control, Adhesion Control, Negative Pressure Adhesion

1. Motivation and State of the Art

Safety is a main requirement for all kind of robots. In most cases the developers pay attention to the operation safety to ensure that the system will not harm people or damage something.[1] Regarding climbing robots the most endangered object is the robot itself. In general the threat caused by climbing robots[2–7] is nearly zero because they are slow and do not interact with humans. Only a drop-off of the robot is dangerous and should be avoided under all circumstances.

Therefore, a behavior-based adhesion controller has been developed which consists of individual, but interacting components to reduce or avoid robot slip and tilt – which are main threats for climbing robots. By this structure, we are able to use the advantages of a behavior-based network in combination with several closed-loop controllers and operation modules:

The control system can be built and enhanced bottom-up, the behavior meta data can be used as additional virtual sensor information.

As test platform we use the climbing robot CROMSCI (fig. 1) which has been developed for inspections of large concrete structures. The system combines several innovative techniques like a negative pressure adhesion system with multiple chambers and a reservoir, adaptive sealings in the shape of spokes and a drive system with integrated load cells.[8] For inspection tasks a manipulator arm can be mounted to carry the inspection sensors. An umbilical cable connects the robot to a supply station.

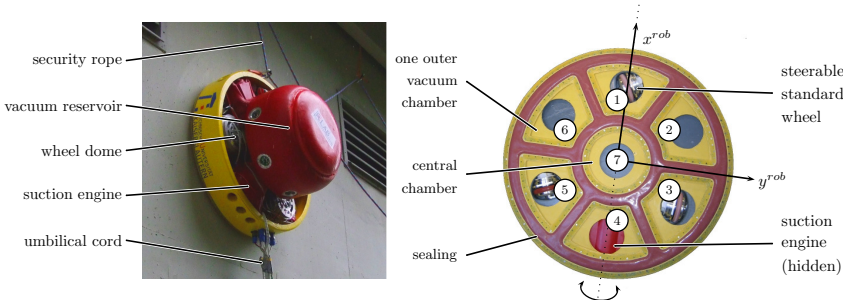

Fig. 1. Climbing robot CROMSCI in action (left) and the setup of the seven-chamber adhesion system (bottom view, right)

2. Behavior-Based Control Architecture iB2C

The negative pressure control system as presented by Hillenbrand *et al.*[9] has been transfered into a behavior-based network in which several individual controllers, limiters and calculation units interact. Each of these behaviors follows the design of the iB2C[a] architecture by Proetzsch *et al.*[10]

In general, one differs between behavior and fusion modules (see fig. 2). Behaviors are algorithmic elements generating outputs from given inputs. Fusion modules combine these outputs, if two or more behaviors try to control the same resource. Each behavior generates control data $\vec{u}$ based on an arbitrary transfer function $F(\vec{e}, \iota)$ which uses the given input vector $\vec{e}$ and its *activation* $\iota = s \cdot (1 - max_{1..n}(i))$ (maximum possible activity). A standardized interface allows to influence other modules and to signal the current behavior state: *stimulation* $s \in [0, 1]$ (activates the behavior),

[a]iB2C stands for *Integrated Behaviour-Based Control* and can be downloaded on `http://rrlib.cs.uni-kl.de/mca2-kl/libraries/ib2c/`

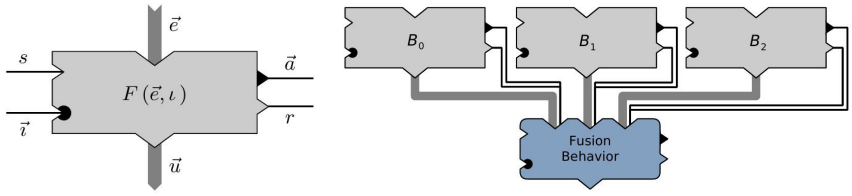

Fig. 2. Behavior module in the behavior-based architecture iB2C (left) and an exemplary fusion of the outputs of three behaviors by taking meta data into account (right)

inhibition $\vec{i} \in [0,1]^n$ (reduces stimuli), *activity* $\vec{a} \in [0,1]^m$ (real amount of action it performs) and *target rating* $r \in [0,1]$ (dissatisfaction in the current situation). The advantage of this architecture is that additional meta data will be received which can be used for behavior interaction and data fusion to implement a very complex system behavior based on many individual units. Behaviors and fusion modules can be encapsulated to behavior groups for a better survey. It has to be mentioned that the iB2C architecture scales from the reactive level up to high-level functions.

3. Control Behaviors

The novel behavior-based adhesion control system consists of different control levels as illustrated in fig. 3. The following list shows, which behaviors are used to control the adhesion and how the meta data *activity* and *target rating* for behavior interaction are calculated.

Chamber Controller (CCi) A basic pid closed-loop pressure controller for one working chamber $i \in \{1,2,...7\}$ which exists seven times within the network. The *activity* $a_i^{CC} = \iota_i^{CC} \cdot A_i^{act}/A^{max}$ depends on the actual valve area A_i^{act} and its maximum. In colloquial speech, this points out that the behavior is more active if the valve is opened. The *target rating* $r_i^{CC} = \left|p_i^{act} - p_i^{des}\right| / \Delta p^{max} + \left(1 - \iota_i^{CC}\right)$ uses the difference of desired p_i^{des} and actual chamber pressure p_i^{act} and therefore is unhappy if the desired pressure value can not be reached or if the behavior is not activated.

Chamber Deactivator (CDi) A deactivator surveys one working chamber and inhibits the corresponding CCi in cases of high leakages. By this means the chamber is cut off from the adhesion system to prevent a global fail. Additionally, the deactivator tests the leak chamber before it is reintegrated. The *activity* $a_i^{CD} = \iota_i^{CD} \cdot s_i^{act}$ is determined by the chamber state $s_i^{act} \in \{0,1\}$ which depends

on an internal state and the estimated leakage. It is active if the leakage limit has been exceeded and a waiting or testing cycle is started. The *target rating* $r_i^{CD} = s_i^{act} + \hat{A}_i^{leak}/A^{max}$ also depends on the estimated leakage $\hat{A}_i^{leak}$. Therefore, it is dissatisfied if the leakage area tends towards the valve area or if it has to be active.

Chamber Deactivator Control (CDC) This behavior coordinates the individual chamber deactivators to prohibit simultaneous testing of chambers. Additionally, it inhibits the inactive CDi behaviors if the maximum number of inactive chambers nic^{max} has been reached to prevent the cut-off of more chambers. The *activity* $a^{CDC} = \iota^{CDC} \cdot nic/nic^{max}$ increases with the amount of inactive chambers nic. The *target rating* increases with the amount of unhandled leakage: $r^{CDC} = max_{i\in\{1,2,...7\}}(r_i^{CD} \cdot \iota_i^{CD})$.

Manual Chamber Control (MCC) Via this behavior the seven chambers can be activated and controlled individually by hand. These manual values are fused with the calculated ones from the CPC. *Activity* and *target rating* are $a^{MCC} = \iota^{MCC}$ and $a^{MCC} = 0.5$.

Chamber Pressure Calculator (CPC) This behavior calculates individual chamber pressures based on a desired total downforce. Here, the *activity* is equal to the *activation* $a^{CPC} = \iota^{CPC}$, the *target rating* depends on the possible and desired downforce values and on the position of the downforce point: $r^{CPC} = max\left(\left|F_z^{pos} - F_z^{des}\right|/\Delta F^{max}, \left|\vec{P}_F^{pos} - \vec{P}_F^{des}\right|/\Delta P_F^{max}\right)$. Thus, the behavior is dissatisfied if the desired downforce value can not be reached by the adhesion system. This can happen in cases of leakages or 'unusual' settings.

Manual Force Control (MFC) This behavior is used to set a desired total downforce for the negative pressure system. Again, the *activity* is set to the internal *activation* $a^{MFC} = \iota^{MFC}$, whereas the *target rating* is calculated similar to the CPC: $r^{MFC} = max\left(\left|F_z^{act} - F_z^{des}\right|/\Delta F^{max}, \left|\vec{P}_F^{act} - \vec{P}_F^{des}\right|/\Delta P_F^{max}\right)$ by comparing the actual and desired adhesion force values.

Force Controller (FC) This is the high-level closed-loop controller for regulating the downforces at the three wheels which takes the load cell values into account. *Activity* is set to $a^{FC} = \iota^{FC}$, *target rating* again depends on the actual and desired values — but now determined by the load cells (LC): $r^{FC} = max\left(\left|F_{LC,z}^{act} - F_{LC,z}^{des}\right|/\Delta F_{LC}^{max}, \left|\vec{P}_{LC,F}^{act} - \vec{P}_{LC,F}^{des}\right|/\Delta P_{LC,F}^{max}\right)$.

4. Behavior-based Adhesion Control

As important as the individual components is the interaction of them. Figure 3 shows the connections between the different control and fusion behaviors within our iB2C framework. The bottom-layer consists of the *chamber control group* with the seven *chamber control* (CCi) modules and the *chamber deactivator group* with the *chamber deactivator control* (CDC) and *chamber deactivator* (CDi) behaviors. The controller outputs of the CCi behaviors are the desired valve positions to control the air flow between negative pressure reservoir and working chamber. The CDC output is connected to the inhibition inputs of the CDi modules. The CDi *activity* outputs again are used to inhibit the corresponding CCi. All these different controlling behaviors work in parallel.

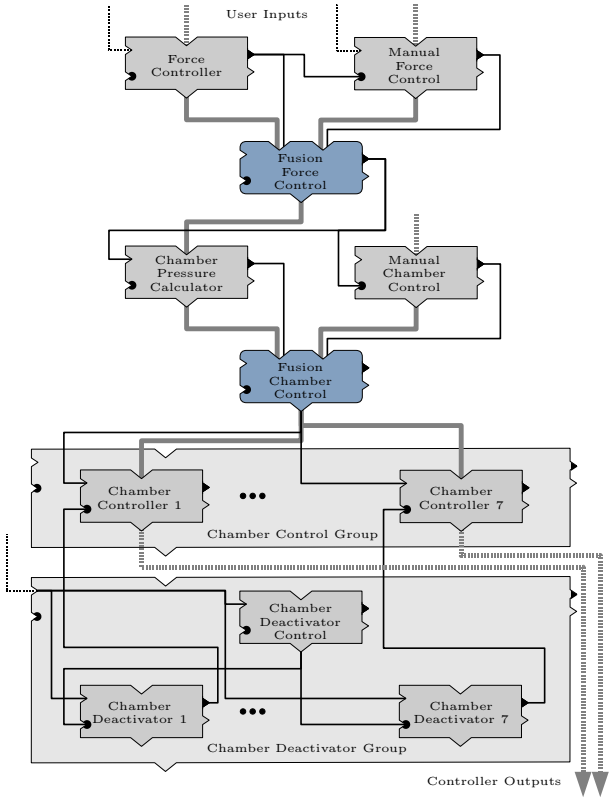

Fig. 3. Overall behavior structure of the negative pressure and force control system. The user can activate additional functionalities by stimulating the behaviors *force controller*, *manual force control* and the *chamber deactivator group*.

In the middle of fig. 3 the *manual chamber control* (MCC) and *chamber pressure calculator* (CPC) are located, a fusion module combines their controller outputs. The MCC can be used for additional manual control settings like a position control of the chamber valves. The CPC receives the desired force values from the *fusion force control* on top. This fusion module stimulates the CPC and inhibits the MCC via its *activity*. The incoming force values are taken either from the *force controller* (FC) which uses the load cell values or from the *manual force control* (MFC) which is inhibited by FC's *activity*. It is obvious that this structure allows only one of the higher behaviors to control the adhesion because of the different user commands which are possible: The FC works on desired loadcell force values, the MFC takes the desired adhesion force and the MCC either uses individual valve positions or chamber pressures. The user can now activate FC, MFC and CDC depending on the desired system functionalities and set the corresponding control values.

5. Experiments and Test Results

Figure 4 gives an overview on how the individual components interact. On the left, *activity* (darkgray) and *activation* (lightgray) are given. On the right, one can find the *target rating* of each behavior (because of page limits the individual behaviors of chambers 4-7 are not shown). In this setup the simulated robot drives downward a wall facing a deep crack.

At the beginning, the MCC is active with the same desired chamber pressure for all chambers. Therefore, robot tilt is not balanced out which results in a x-position of the downforce point $P^{act}_{LC,x}$ of $0.042[m]$ (bottom right graph). Then the user stimulates MFC and FC. Finally, the FC is active and uses the desired downforce $F^{des}_{LC,z} = 2200[N]$ while MFC and MCC are inhibited ($a^{MFC} = a^{MCC} = 0$). Now the robot tries to overcome the crack but the leakages are too high: CD1, CD2 and CD6 become active and shut down the frontal chambers (compare fig. 1) by inhibiting CC1, CC2 and CC6 – the light gray *activation* graphs go down to zero. Because of the maximal amount of inactive chambers the CDC is full active ($a^{CDC} = 1$) and inhibits CD3, CD4, CD5 and CD7, no more chambers can be shut down. After some time the CDC starts a testing cycle of CC1 which fails because the chamber is still influenced by the crack. The minimum downforce in this period is at about $1760[N]$ provided by the four remaining chambers. The x-coordinate of the downforce moved to $-0.082[m]$ which is still within the stability triangle – the robot does not tilt. Now the robot is driven backward, the CDi behaviors become inactive again and the system can recover.

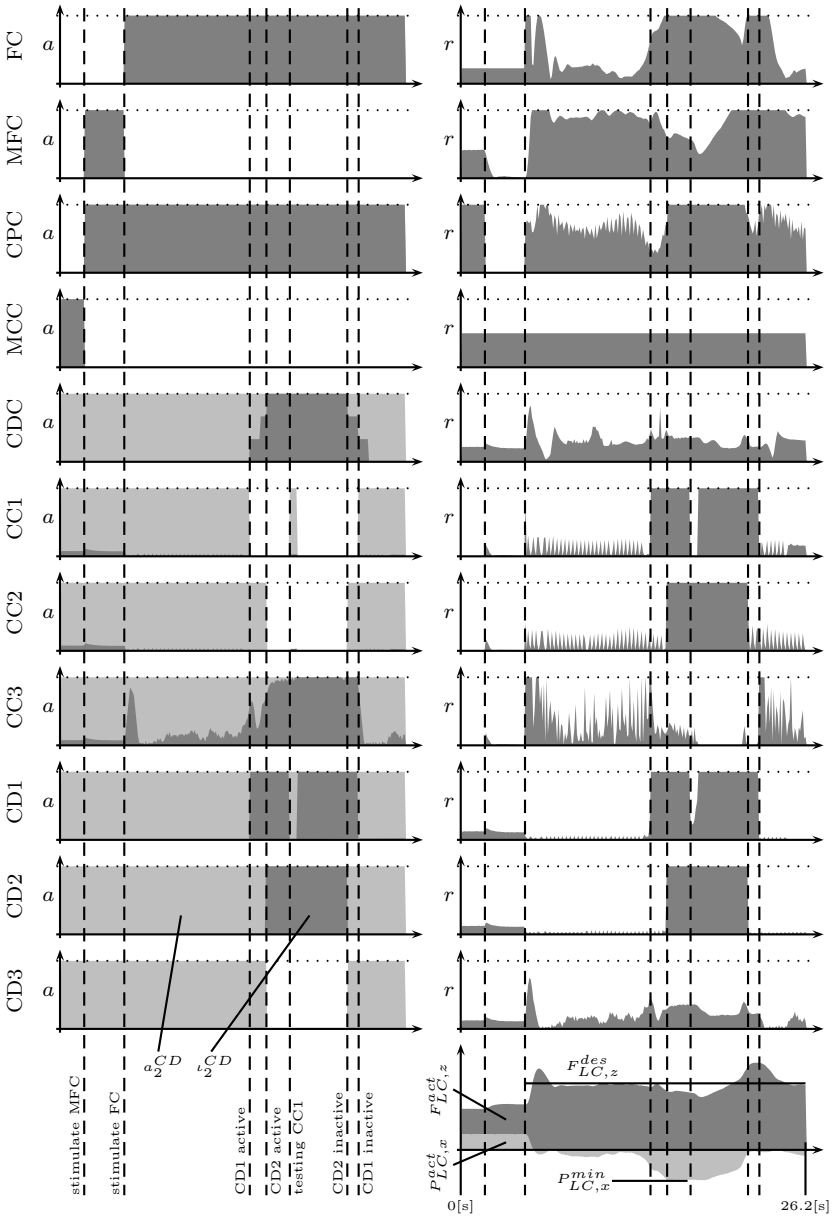

Fig. 4. Plot of behavior *activities a* (left, gray), *activation* (left, light gray) and *target ratings r* (right). On bottom right one can find the resulting downforce $F^{act}_{LC,z}$ (dark gray graph) with a desired force of $F^{des}_{LC,z} = 2200[N]$. The light gray graph indicates the x-position of the downforce point which reaches a minimum of $P^{min}_{LC,x} = -0.082[m]$.

6. Conclusion and Outlook

We presented the novel behavior-based network for climbing robots which uses individual components based on the iB2C architecture to perform a cascaded closed-loop adhesion control. Meta data are used for behavior interaction and will be used in future for additional controlling and evaluation of the system state. By this generality it is easy to integrate additional components to the control system, to reuse them in other contexts and to perform analyses. The functionality and the performance of this system have been proved by experiments. The future work is now focused on an evaluation of the behaviors for risk estimation and prediction.

References

1. G. R. Ward and S. R. G.Went, Robot safety, in *Industrial Robot: An International Journal*, (1) 1995 pp. 10–13.
2. F. Bonaccorso, D. Longo and G. Muscato, Modelling of an innovative actuator for climbing robot adhesion, in *12th International Conference on Climbing and Walking Robots (CLAWAR)*, September 2009.
3. T. Hayakawa, T. Nakamura and H. Suzuki, Development of a wave propagation type wall-climbing robot using a fan and slider cranks, in *12th International Conference on Climbing and Walking Robots (CLAWAR)*, September 2009.
4. H. Prahlad, R. Pelrine and S. Stanford et al., Electroadhesive robots - wall climbing robots enabled by a novel, robust and electrically controllable adhesion technology, in *International Conference on Robotics and Automation (ICRA)*, May 19-23 2008.
5. J. Shang, B. Bridge, T. P. Sattar, M. S and A. Brenner, Development of a climbing robot for inspection of long weld lines, in *Climbing and Walking Robots*, July 2007.
6. M. J. Spenko, G. C. Haynes, J. A. Saunders, M. R. Cutkosky, A. A. Rizzi, R. J. Full and D. E. Koditschek, *Journal of Field Robotics* **25** (2008).
7. H. X. Zhang, W. Wang and J. W. Zhang, High stiffness pneumatic actuating scheme and improved position control strategy realization of a pneumatic climbing robot, in *IEEE International Conference on Robotics and Biomimetics (ROBIO)*, February 2009.
8. D. Schmidt, C. Hillenbrand and K. Berns, Omnidirectional locomotion and traction control of the wheel-driven, wall-climbing robot, cromsci, in *Robotica Journal (First View)*, (Cambridge University Press, 11th April 2011).
9. C. Hillenbrand, D. Schmidt and K. Berns, Cromsci - development of a climbing robot with negative pressure adhesion for inspections, in *Industrial Robot Volume 35 Issue 3*, (Emerald Group Publishing Ltd., May 13 2008).
10. M. Proetzsch, T. Luksch and K. Berns, Development of complex robotic systems using the behavior-based control architecture iB2C, in *Journal of Robotics and Autonomous Systems*, January 2010 pp. 46–67.